Analyzing Network Composition: From Links to Clusters to Connectivity

Simon Heimlicher
Computer Engineering and Networks Laboratory
ETH Zurich, Switzerland

Kavé Salamatian
LISTIC PolyTech
Université de Savoie Chambery Annecy, France

***Abstract*—For a set of nodes to turn into a network, physical links need to be composed to paths. If the link graph is connected, full connectivity may be achievable through a simple routing algorithm. In scenarios with partitioned link graph, opportunistic forwarding algorithms may leverage paths segments to—over time—enable communication between disconnected nodes. The composition of such logical paths satisfying the requirements of the application, and the extent to which logical connectivity is achieved, is of great interest in such scenarios. In this paper, we look at network composition via the connected components (clusters) evolving in the logical connectivity graph as a function of the statistics of the physical link graph as well as the delay tolerance of the application. We model a network as a Markov process describing the sizes of clusters evolving through merge and split reactions. Complementing previous analysis of the stationary state, we now analyze the transient. Further, we study the fluctuation of the cluster size of an individual node over time and show how the current can predict the future size. Further, we study network composition by opportunistic forwarding and the attained level of connectivity as a function of buffering duration. Comparison with real-world contact and mobility traces with dozens to thousands of nodes confirms the validity of the model.**

I. Introduction

A minimal requirement for a set of N nodes to constitute a network is that some of them be connected by a set of links. These links correspond to communication opportunities at some time t and together with the set of nodes define the physical link graph. But while links are the physical substrate for connectivity, it is the paths composed from those links that make a network through the routing algorithm and provide a well-defined communication service through the transport protocol. A network is called *connected* if between every pair of nodes a path, *i.e.*, a connected sequence of links, exists. This definition of connectivity is appropriate when it corresponds to satisfying the requirements of an application to run between those nodes. (Although one might want to consider only paths that can be determined by the routing protocol and used for end-to-end communication by the transport protocol.) In this classical sense, we define network composition simply as the process of determining paths between all nodes based on the link graph.

In practice, however, the link graph may be partitioned into a collection of connected components, or *clusters*. In this case, the important question is whether a given application may still run between all or a subset of nodes. In [1], we studied this question using an analytical model of the cluster size distribution in stationary state. The stationary distribution characterize in detail the physical topology of a network. Further it indicates to what extent multi-hop paths may provide shortcuts for forwarding between nodes in disjoint clusters.

In this paper we build upon this work and analyze the transient behavior of network composition and the dynamics of individual nodes in partitioned networks. To recapitulate, the model describes a network as a set of clusters that merge and split in analogy to how globs of particles coalesce and fragment in a solvent. The state of this stochastic system is described by the cluster size vector, whose ith element denotes the number of clusters of size i at time t, with $i = 1, 2, \ldots, N$. The state may change through two primitive transitions: two clusters merging into one, or one cluster splitting in two. These transitions define a Markov process over the finite state space of all partitions of the number of nodes. While [1] considers only the stationary state of the process, we now complement this work by an extensive analysis of transient and dynamic properties. We will show how the process can be replaced by an equivalent pure merging process, which will enable us to derive analytically the duration of convergence from a set of isolated nodes to the stationary cluster size distribution, giving direct insight as to the speed of network composition.

The variation of the network partition over time may enable communication through opportunistic forwarding, which—albeit incurring delay, overhead, and loss—may be the only way to transfer information. We will analyze the variation of the cluster size of an individual node to gain further understanding of the temporal variation of the network topology. This also enables predicting the future size of a cluster, which may help governing forwarding decisions.

In disconnected scenarios, the link graph sets hard physical limitations, but there are other factors that may preclude connectivity, such as energy constraints or privacy concerns. No matter the reason, in disconnected networks it may be of more interest whether two nodes are able to run a given application, rather than whether they are connected in the classical sense. While for real-time applications only node pairs connected via low-delay paths may be of interest, an application that distributes the latest episode of a podcast through randomized broadcasting may well consider all nodes which receive the data within a few hours to be connected. In light of this, we define a *logical path* as a sequence of links that—possibly over the course of time—enable interaction between nodes *in*

the terms of the application. A network is *logically connected* if between every pair of nodes a logical path exists. Logical network composition is thus an application-specific process that composes logical paths from physical links.

The composition of such logical paths given the link graph is the optimization problem to be solved by routing and transport layers as a function of the target application. More formally, the aim is to determine the optimal composition relation defined over the link graph. What is considered optimal depends on the particular application of the network; for example one might assume node i to be connected to a node j if they can exchange information at a minimal rate, or with a bounded delay. More generally, two nodes may be considered to be connected if the state of node i may impact the state of node j. In general the composition relation is not necessarily symmetric or transitive, *i.e.*,, if node i is connected to node j, this does not imply the inverse; and node i being connected to node j and node j being connected to node k does not imply that node i is also connected to node k. As an example of the non-transitivity, consider logical connectivity defined via a bounded delay.

Yet, even under logical connectivity, a network scenario may be connected only intermittently or remain partitioned. Intermittent connectivity may be due to network growth or temporal disruption of links due to outages and energy saving efforts. In all those cases, understanding the *limits of logical connectivity* is of major interest. For example in delay-tolerant networking (DTN) logical connectivity is often limited by the buffer size available at intermediate nodes. But while increasing the retention period of messages to be forwarded may improve logical connectivity, there is a critical value after which logical connectivity plateaus and only buffer requirements increase. We will demonstrate this effect using a simple opportunistic forwarding scheme and see that, indeed, there is a critical delay of diminishing return. This critical delay is of great importance for the design and operation of opportunistic forwarding schemes.

We validate our analytical results against real-world mobility traces from conference visitors and taxicabs, from which we extract merge and split rate to calibrate our model. We then compare the predicted behavior with the empirical results from the traces and in general observe very good agreement.

Our work applies very generally to network composition as the evolution of a network from isolated nodes to a large-scale connected topology. Though this was studied using degree distribution or clustering coefficient as metrics, we argue that the cluster size distribution may yield additional insight. But due to space limitations this must be postponed to future work.

Summarizing main contributions, we build upon our model of clustering and use it to predict analytically

- the duration of the transient from isolated nodes to the stationary cluster size distribution, and
- the future size of the cluster of an individual node given the current size in stationary state.

We apply the proposed concept of logical connectivity to study

- the level of logical connectivity provided by opportunistic forwarding as a function of buffering duration.

All analytical results are validated against real-world traces:

- contact trace from Infocom 2005 (41 nodes), and
- mobility traces from taxicabs in San Francisco (536 nodes) and Shanghai (4063 nodes) based on GPS.

We further discuss logical connectivity in the next section. In Sec. III we extend the merge–split model to analyze its transient behavior in Sec. IV and the dynamics of individual nodes in Sec. V. Section VI outlines calibration of the model to empirical data, which is then used for extensive validation against traces in Sec. VII. Finally, Section VIII discusses related work and Sec. IX concludes the paper.

II. Opportunistic Forwarding

Before diving into the mathematical analysis, let us introduce the opportunistic forwarding paradigm that will serve as an example application of the theory we will present. In delay-tolerant networking (DTN), the route of a message from source to destination cannot be determined a priori as communication is only enabled through *opportunistic forwarding* [2]. This means that communication opportunities, or *contacts,* are seized by the forwarding algorithm at intermediate nodes depending on the limited information available. To model such an algorithm, we define a node i to be logically connected to node j with buffering duration D, if buffering the message at intermediate nodes for D units of time may yield a sequence of communication opportunities for the message to reach node j. While this yields only an upper bound on the fraction of nodes that are able to communicate, this logical connectivity relation has the advantage of being both symmetrical and transitive. In Sec. VII-D, we will study the size of logical clusters generated by this algorithm as a function of D. This illustrates the use of the theoretical model to gauge the impact of buffering duration, which is of great interest for the operation of opportunistic forwarding schemes.

III. Analytic Formulation

In this section we briefly review the merge–split process for clustering in mobile networks we introduced in [1], before we go on to analyze the transient and convergence properties.

A. Finite size system formulation

We describe an arbitrary network as a system of N interacting nodes. At every time t, a node is in exactly one logical cluster, *i.e.*, it is member of a set of nodes that are logically connected as defined by the logical connectivity relation at time t. The state of the system is described by the cluster size vector, a finite vector denoted as $(\eta_N(1,t), \eta_N(2,t), \ldots, \eta_N(N,t))$ whose elements $\eta_N(i,t)$ hold the number of clusters of size i at time t.

Two primitive reactions occur between clusters.

1) **Merge reaction:** A cluster of k nodes merges with a cluster of l nodes, yielding a cluster of $k+l$ nodes:

$$C_k + C_l \to C_{k+l}.$$

This reaction is also called *coalescence* and happens at a rate $\psi_N(k,l)$, which is assumed to be symmetric, *i.e.*, $\psi_N(k,l) = \psi_N(l,k)$. A merge reaction of clusters of sizes k and l has the following drift effect on the cluster size vector: $(\ldots, \eta_N(k,t) - 1, \ldots, \eta_N(l,t) - 1, \ldots, \eta_N(k+l,t) + 1, \ldots)$.

2) **Split reaction:** A cluster of size l splits into two clusters of sizes k, $(k < l)$ and $l - k$:

$$C_l \to C_k + C_{l-k}.$$

This reaction is also called *fragmentation* and happens at a rate $\phi_N(l|k)$ and we assume $\phi_N(l|k) = \phi_N(l|l-k)$. A split reaction has the following drift effect on the cluster size vector: $(\ldots, \eta_N(l-k,t)+1, \ldots, \eta_N(k,t)+1, \ldots, \eta_N(l,t) - 1, \ldots)$.

We will drop subscript N when it is obvious from context. These reactions happen subject to the node conservation condition:

$$\sum_{k=1}^{N} k\eta_N(k,t) = N, \forall t \leq 0. \tag{1}$$

This defines a Markov process over the finite state space $\Omega = \Omega_N = \{\tau\}$ of all partitions of N we call a *merge–split process.* A special case of this process with only the merge reaction is called a Marcus-Lushnikov process [3], [4] and has gained attention from the mathematical community. The analogous process involving only the split reaction is called fragmentation process and has been studied extensively in the context of branching processes. The problem we analyze here is a mix of these two problems.

Further, we define the *intensity ratio* as a function $q(k,l)$, based on the ratio between merge and split intensity:

$$q(k,l) = \begin{cases} \dfrac{\psi(k,l)}{\phi(k+l|l)}, & \text{if } \psi(k,l)\phi(k+l|l) \neq 0 \\ 0, & \text{otherwise} \end{cases} \tag{2}$$

In previous work [1], we studied the equilibrium behavior of a case where the process is reversible, *i.e.*, the case where for some function $a(k) > 0,\ k = 1, \ldots, N$, $q(k,l)$ can be written as

$$q(k,l) = \frac{a(k+l)}{a(k)a(l)}. \tag{3}$$

We also presented a procedure for deriving the exact stationary distribution of cluster size $\eta_N(k)$, the mean number of clusters of size k at the stationary state, as a function of $a(x)$. However we showed that this exact derivation becomes imprecise for large N because of numerical problems related to representation of very large numbers. In order to deal with this problem, we developed a mean field approximation by studying the convergence of the above defined merge–split process as the number of interacting nodes becomes large and obtained a closed-form formula. We will briefly repeat the asymptotic result as it will be used in the dynamical analysis in Sec. V. Note that in this case one needs to ensure that the physical conditions are preserved by holding the density of nodes constant. We achieve this by letting the volume $V(n)$ grow along with the number of nodes n diverging, while keeping node density equal to N. Along these lines, we define $\eta(k,t)$ as the density of clusters of size k at time t and $K(k,l)$ $(F(k|l))$ as the merge (split) rate per unit volume.

When the number of interacting particles grows, we need to ensure that the physical conditions are preserved by keeping the density of nodes constant while the number of nodes diverges. Assume that a finite system with n nodes is evolving in a unit volume. In order to maintain the same physical conditions, we have to let the volume $V(n)$ grow along with the number of nodes n diverging while holding node density equal to N, *i.e.*, we analyze $\eta_N(k)$, the density of clusters of size k, when the node density is equal to N:

$$\lim_{n\to\infty, n=N.V(n)} \eta_n(k) = \eta_N(k),$$

where the constraint $n = N.V(n)$ results from the node density being set to N.

By extension $\eta(k,t)$ is defined as the density at time t of clusters of size k. that contains up to a proportion $x = \frac{k}{N}$ of all nodes. We also define the merge rate per volume unit as

$$K_N(k,l) = \lim_{n\to\infty, n=N.V(n)} \frac{\psi_n(k,l)}{V(n)}.$$

Similarly we define the split rate per volume unit as

$$F_N(k|l) = \lim_{n\to\infty, n=N.V(n)} \frac{\phi_n(k|l)}{V(n)}.$$

Also for these quantities, we will drop index N in the sequel.

Under such conditions we formally proved in [1] that the correlation between the cluster sizes vanishes as the *propagation of chaos* phenomenon manifests itself. This results in the convergence of the merge–split process to a mean field that is defined as the solution of the Kolmogorov forward equation for the Markov chain governing the merge–split process with infinite number of nodes:

$$\begin{aligned} \frac{\partial \eta(m,t)}{\partial t} = & \frac{1}{2}\sum_{l=1}^{m-1} K(l, m-l)\cdot\eta(l,t)\eta(m-l,t) \\ & - \sum_{l=1}^{\infty} K(m,l)\cdot\eta(m,t)\eta(l,t) \\ & + \sum_{k=m+1}^{\infty} F(k|m)\cdot\eta(k,t) \\ & - \frac{1}{2}\sum_{l=1}^{m-1} F(m|l)\cdot\eta(m,t). \end{aligned} \tag{4}$$

where $\eta(k,t)$ is the mean number of clusters of size k at time t and the functions $K(m,l)$ and $F(k|m)$ are, respectively, the mean merge rate per volume unit and the mean split rate per volume unit. We assume that the initial state $\eta(m,0),\ m = 1, \ldots, \infty$, satisfies the node conservation condition, *i.e.*,

$$\sum_{k\geq 1} k\eta(k,0) = N;$$

with the density of nodes being equal to N.

There are two special cases of interest here: discarding the split reaction ($F(k|l) = 0$ for all $k < l$) yields a purely coalescent process described by the *Smoluchowski equation* [5]. Discarding the merge reaction ($K(k,l) = 0$ for all k, l) yields a pure branching process. The Smoluchowski equation enjoys a large interest in statistical physics [6], where it is used to analyze a large number of real-world scenarios (polymer synthesis, aerosol formation in the atmosphere, or phase separation in liquid mixtures). More recently through the survey by D. J. Aldous [7], it gained traction in mathematics.

The solution of (4), when it exists, has a unique stationary and stable solution $\eta_N(k,t)$, *i.e.*, ${}^{\partial\eta(k)}/_{\partial t} = 0$, and provides a mean field approximation (MFA) to the stationary distribution of cluster size in the network. The stationary MFA, *i.e.*, the distribution where ${}^{\partial\eta(k,t)}/_{\partial t} = 0$, is denoted as $\eta(k)$. We showed in [1] that for reversible processes this stationary distribution has the following simple closed form:

$$\eta(k) = a(x)e^{\lambda x}, \tag{5}$$

where $a(x)$ is the function controlling the intensity ratio and λ is chosen so that the node conservation constraint (1) holds.

This is remarkable as it relates a microscopic property of the merge–split process, the function $a(x)$ controlling the intensity ratio, to a macroscopic property of the process, the stationary distribution of cluster size $\eta(k)$.

In this paper, in contrast to [1] dealing with the asymptotic stationary behavior, we analyze the dynamics of the merge–split process. In particular we will study the transient behavior before stationary state. Further, we will analyze the temporal fluctuation of the size of the cluster of an individual node.

IV. Transient Analysis

In order to study the transient behavior of the system, we need to solve (4). Before going further, note that the function $\eta(i,t)$ does not strictly define a probability distribution function (PDF) for the cluster density because $L_0(t) = \sum_{k=1}^{\infty}\eta(k,t)$ might not equal one. In fact, $L_0(t)$ represents the mean number of clusters at time t. With this definition, the PDF of cluster size (varying over time) is given by

$$\mathbb{P}[(i,t)] = \frac{\eta(i,t)}{L_0(t)} \tag{6}$$

The value $L_1(t) = \sum_{k=1}^{N} k\eta(k,t)$ is the global node density and is assumed to be constant due to the node conservation condition. Note that if nodes vanish, are created, or are removed from the merge–split process by being trapped under certain physical conditions, $L_1(t)$ may vary with time. In the sequel, we assume that the process has been rescaled such that the initial node density is equal to one, *i.e.*, $L_1(0)$ (resulting in $L_0(t) \leq 1$).

A. Purely coalescent model

By discarding the split reaction, we obtain a purely coalescent equation called the Smoluchowski equation [5].

$$\frac{\partial\eta(m,t)}{\partial t} = \frac{1}{2}\sum_{l=1}^{m-1} K(l, m-l)\cdot\eta(l,t)\eta(m-l,t) - \sum_{l=1}^{\infty} K(m,l)\cdot\eta(m,t)\eta(l,t) \tag{7}$$

The purely coalescent equation is interesting *per se*, as the splitting can be inexistant or very infrequent in some case, *e.g.*, when analyzing the topology of a wired network, subnetworks may merge into larger networks but generally do not split (unless a link failure occurs).

A large body of literature has studied this equation under various assumptions on the form of the merge rate (see [6], [7] for a survey of existing results). In the forthcoming we will describe in detail a particular case with a closed-form solution; the constant kernel, where $K(x,y) = K_0$.

B. Analytic solution for constant merge rate $K(x,y) = K_0$

Even though the constant merge rate is the simplest case, it has a practical interpretation, *e.g.*, if the volume of the "connectivity sphere" around nodes and clusters is negligible, one can assume that the merge rate is constant. This approximately holds in very sparse mobile networks with infinite buffer space; this case will be studied in detail in Sec. VII-D.

The solution of the Smoluchowski equation follows a generic method that uses the generating function of the distribution $\eta(k,t)$ defined as:

$$\mathcal{N}(z,t) = \sum_{k=1}^{\infty}\eta(k,t)e^{-kz}.$$

It is straightforward to see that

$$L_0(t) = \mathcal{N}(0,t),\ L_1(t) = \frac{\partial}{\partial z}\mathcal{N}(z,t)|_{z=0}.$$

More generally the function

$$L_k(t) = \frac{\partial^k}{\partial z^k}\mathcal{N}(z,t)|_{z=0}$$

gives the k^{th} moment of the cluster size distribution function.

Using $\mathcal{N}(z,t)$, one can transform the infinite set of coupled ordinary equations in the Smoluchowski equation into the following single Riccati partial differential equation:

$$\frac{\partial\mathcal{N}}{\partial t} = \frac{K_0}{2}\mathcal{N}(z,t)^2 - K_0\mathcal{N}(0,t)\mathcal{N}(z,t). \tag{8}$$

If we now set $z = 0$ in the above equation, we can substitute $\mathcal{N}(z,t) = \mathcal{N}(0,t)$ by $L_0(t)$ and obtain a first-order ordinary differential equation with variable $L_0(t)$; *i.e.*,

$$\frac{dL_0(t)}{dt} = -\frac{K_0}{2}L_0^2(t), \tag{9}$$

Now let us assume that at the beginning all nodes are isolated, in other terms $\eta(1,0) = 1$ and $\eta(k,0) = 0, k = 2,3,\ldots$. This

results in an initial condition $L_0(0) = 1$ (recall that we have rescaled the number of nodes, N, such that $L_1(t) = 1$ for (9)). Hence, the number of clusters evolves over time as:

$$L_0(t) = \frac{2}{K_0 t + 2}, \tag{10}$$

giving the evolution of the number of clusters from 1 to 0 (after rescaling).

Undoing the previous substitution and putting back $\mathcal{N}(z,t)$ for $\mathcal{N}(0,t)$ in (8) yields a Riccati equation that can be solved by the transformation $\mathcal{M}(z,t) = \frac{1}{\mathcal{N}(z,t)}$. Applying this transformation results in a linear equation for $\mathcal{M}(z,t)$. By imposing the initial condition $\mathcal{M}(z,0) = \frac{1}{\mathcal{N}(z,0)} = e^z$, we obtain the solution

$$\mathcal{N}(z,t) = \frac{4e^{-z}}{(K_0 t + 2)^2} \left(1 - \frac{K_0 t e^{-z}}{K_0 t + 2}\right)^{-1}.$$

Finally, expansion of the above term as a power series yields the final solution:

$$\eta(k,t) = \frac{4}{(K_0 t + 2)^2} \left(\frac{K_0 t}{K_0 t + 2}\right)^{k-1}. \tag{11}$$

1) Remarks: The obtained solution may seem complicated but fortunately there is a simple interpretation. Let us define

$$p(t) = \frac{K_0 t}{K_0 t + 2},\ 0 < p(t) < 1 \tag{12}$$

as a probability. Then, using the definition in (6) to derive the time-varying PDF of cluster size, we have $\mathbb{P}(k,t) = (1 - p(t))\, p^{k-1}(t)$. Observe that this is the probability distribution of a Bernoulli trial with probability $p(t)$. One can therefore generate clusters with the density given in (11) by running a Bernoulli trial. A coin with probability of head equal to $p(t)$ is tossed. When a head appears, a node is added to the current cluster. When a tail appears one moves to the next cluster and adds a node to this cluster. The probability of the Bernoulli trial, $p(t)$, changes from $p(0) = 0$ to $\lim_{t\to\infty} p(t) = 1$, *i.e.*, the probability of joining a cluster goes to 1 as time increases. This means that the system converges asymptotically, with $t \to \infty$, to a giant component where all nodes are connected with probability 1.

The merge rate K_0 acts as a time scaling, *i.e.*, the larger K_0 is, the faster $\eta(i,t)$ converges to its limit behavior. In particular, for $K_0 t \gg 1$, we have $p(t) \approx 1 - \frac{2}{K_0 t}$ and

$$\eta(k,t) \approx \frac{4}{(K_0 t)^2} e^{-\frac{2k}{K_0 t}}.$$

This limit behavior gives insight into the form of the cluster size distribution. With increasing t, $2/K_0 t$ becomes smaller and $\exp(-2k/K_0 t)$ remains close to 1 for a larger range of k values, *i.e.*, the distribution of cluster size converges to a uniform distribution with level $2/K_0 t$ and support in the order of $K_0 t/2$. With increasing t, the level of the uniform distribution decreases while its support increases, resulting asymptotically in a single infinite size cluster containing all nodes. Based on the above consideration the stationary distribution $\eta(k,\infty)$ is such that a cluster of any size occurs with the same probability.

The above analysis illustrates the purely coalescent model; however many network scenarios are described better by a merge–split process. In the sequel we provide general conditions under which the distribution of the merge–split process can be derived from the purely coalescent (merge-only) case.

C. Extension to general reversible merge–split processes

Let us assume that the merge–split process under study is a reversible system, *i.e.*, there exists a function $a(\cdot)$ such that its intensity ratio satisfies (3). For such a system, we showed in [1] that it converges to a mean field regime when the number of nodes increases, and that the mean field can be derived by solving the differential equation given in (4). For such systems, the split and merge rates are related through

$$F(m|l) = K(l, m-l)\frac{a(l)a(m-l)}{a(m)}. \tag{13}$$

Using this property one can prove the following theorem.

Theorem 1. *The differential equation given in* (4) *can be rewritten as a Smoluchowski equation relative to a purely coalescent system with a time varying merge rate given as:*

$$K'(m,l) = K(m,l)\left(1 - \frac{a(m)a(l)}{a(m+l)}\frac{\eta(m+l,t)}{\eta(m,t)\eta(l,t)}\right). \tag{14}$$

We call this equation the modulated Smoluchowski equation. *The merge–split process reaches its stationary distribution when $K'(m,l) = 0,\ \forall m,l > 0$,* i.e.*, stationary equilibrium is reached when*

$$\frac{a(m)a(l)}{a(m+l)} = \frac{\eta(m,t)n(l,t)}{\eta(m+l,t)}, \tag{15}$$

and this is the case when $n(k) = a(k)e^{\lambda k}$, as predicted by the mean field approximation.

Proof: Substituting (13) into the merge–split differential equation (4) yields:

$$\begin{aligned}\frac{\partial \eta(m,t)}{\partial t} = {} & \frac{1}{2}\sum_{l=1}^{m-1} K(l,m-l)\eta(l,t)\eta(m-l,t) \\ & - \sum_{k=1}^{\infty} K(m,k)\eta(m,t)\eta(k,t) \\ & + \sum_{k=m+1}^{\infty} K(k-m,m)\frac{a(k-m)a(m)}{a(k)}\eta(k,t) \\ & - \frac{1}{2}\sum_{l=1}^{m-1} K(m-l,l)\frac{a(m-l)a(l)}{a(m)}\eta(m,t).\end{aligned} \tag{16}$$

Changing the bounds of the third summation yields

$$\begin{aligned}\frac{\partial\eta(m,t)}{\partial t} &= \frac{1}{2}\sum_{l=1}^{m-1} K(l,m-l)\eta(l,t)\eta(m-l,t)\\ &\quad -\sum_{k=1}^{\infty} K(m,k)\eta(m,t)\eta(k,t)\\ &\quad +\sum_{k=1}^{\infty} K(m,l)\frac{a(k)a(m)}{a(m+k)}\eta(m+k,t)\\ &\quad -\frac{1}{2}\sum_{l=1}^{m-1} K(m-l,l)\frac{a(m-l)a(l)}{a(m)}\eta(m,t).\end{aligned}$$

This results in

$$\begin{aligned}\frac{\partial\eta(m,t)}{\partial t} &= \frac{1}{2}\sum_{l=1}^{m-1} K'(l,m-l)\eta(l,t)\eta(m-l,t)\\ &\quad -\sum_{k=1}^{\infty} K'(m,k)\eta(m,t)\eta(k,t),\end{aligned} \tag{17}$$

where

$$K'(k,l) = K(k,l)\left(1-\frac{a(k)a(l)}{a(m+k)}\frac{\eta(m+k,t)}{\eta(k,t)\eta(l,t)}\right).$$

This equation is the Smoluchowski equation (7) relative to a purely coalescent process with merge rate $K'(m,l)$. The stationary distribution is reached when $\forall m>0,\ \frac{\partial\eta(m,t)}{\partial t}=0$; this occurs when $\eta(m,t) = a(m)e^{\lambda m}$, as stated in the theorem. ∎

This theorem is conceptually very important as it relates the behavior of a reversible merge–split process to a time-varying purely coalescent process. In the sequel we illustrate this result through an extension of the coalescent model with constant merge rate.

1) Analytic solution for constant merge and split rates: Let us introduce a split component into the purely coalescent model with constant merge rate that was studied in Sec. IV-B. We assume that the intensity ratio defined in (3) is constant and equal to $q(i,j) = {K(i,j)}/{F(i+j|i)} = {K_0}/{2F_0}$. This is compatible with a choice of $a(i) = {2F_0}/{K_0}$ and $F(m|k) = 2F_0$ for all $m > k$. This model is valid when one assumes that clusters of size m split uniformly at a rate F_0 into clusters of smaller sizes, so that $F(M|m) = 2F_0,\ M > m$ (there are two ways of generating a cluster of size m; a split into clusters of size m and $(M-m)$, or *vice-versa*, each happening with a rate F_0). The above assumptions are applicable for instance when nodes are connected through a one-dimensional chain and every link of the chain is broken at the same rate F_0.

For such a merge–split process the mean field equation becomes:

$$\begin{aligned}\frac{\partial\eta(m,t)}{\partial t} &= \frac{K_0}{2}\sum_{l=1}^{m-1}\eta(l,t)\eta(m-l,t)\\ &\quad -K_0\sum_{l=1}^{\infty}\eta(m,t)\eta(l,t)\\ &\quad -F_0(m-1)\eta(m,t)\\ &\quad +2F_0\sum_{k=m+1}^{\infty}\eta(l,t).\end{aligned} \tag{18}$$

This equation can be solved with the following trick: assume that its solution has the same functional form (as a function of $p(t)$) as the purely coalescent case derived before, *i.e.*,

$$\eta(k,t) = (1-p(t))^2\,(p(t))^{k-1},\ \text{for some},\ p(t). \tag{19}$$

Putting this back into (18) leads to an equation where the variable is $p(t)$. For the purely coalescent case, we proved earlier that $p(t) = {K_0 t}/{K_0 t+2}$ and $L_0(t) = (1-p(t))$.

By putting back the value of $\eta(k,t)$ as a function of $p(t)$ (given in (19)) in merge–split equation (18):

$$\begin{aligned}\frac{\partial\eta(k,t)}{\partial t} &= \frac{\partial\eta(m,t)}{\partial p(t)}\cdot\frac{\partial p(t)}{\partial t} = \eta(k,t)\left(\frac{k-1}{p}-\frac{2}{1-p}\right)\frac{\partial p}{\partial t}\\ &= \eta(k,t)\left(\frac{k-1}{p}-\frac{2}{1-p}\right)\left[K_0\frac{(1-p)^2}{2}-F_0 p\right]\end{aligned} \tag{20}$$

where the first line of the equality comes from evaluating $\frac{\partial\eta}{\partial p}$ and the second from inserting (19) into (18).

Looking at equation (20), a differential equation for $p(t)$ can be derived as:

$$\begin{aligned}\frac{\partial p}{\partial t} &= \left[K_0\frac{(1-p)^2}{2}-F_0 p\right]\\ p(t) &= \frac{F_0}{K_0}\frac{r_+-\kappa(t)\cdot r_-}{1+\kappa(t)},\end{aligned} \tag{21}$$

where

$$\begin{aligned}r_\pm &= \left(1+\frac{K_0}{F_0}\right)\pm\sqrt{1+\frac{2K_0}{F_0}}\\ \kappa(t) &= -\frac{r_+}{r_-}e^{-\sqrt{1+\frac{2K_0}{F_0}}t}\end{aligned}$$

By putting back the value of $p(t)$ in (19) we obtain the cluster concentration $\eta(k,t)$ for the merge–split process. The interpretation as a Bernoulli trial with a probability $p(t)$ is still applicable for the purpose of interpretation.

The merge–split system reaches equilibrium when ${\partial\eta(k,t)}/{\partial t} = 0$ for all k. This means:

$$\frac{F_0}{K_0} = \frac{(1-p_\infty)^2}{2p_\infty}$$

This quadratic equation has two roots, one greater than 1, which is incompatible with the definition of probability, and one less than 1, which is given below:

$$p_\infty = \left(1+\frac{F_0}{K_0}\right)-\sqrt{\left(1+\frac{F_0}{K_0}\right)^2-1}. \tag{22}$$

An equilibrium state exists even if the merge and split rates are vastly different.

If splitting dominates, *i.e.*, $\frac{F_0}{K_0} \gg 1$, then $p \ll 1$ and there are very few clusters of large size k (in the limit, almost all nodes are isolated).

If merging dominates, *i.e.*, $\frac{F_0}{K_0} \ll 1$, then $p \to 1$ and the distribution spectrum tends to a stationary distribution, *i.e.*,

$$\eta(k,t) = \frac{(1-p)^2}{p} p^k,$$

hence

$$\frac{2F_0}{K_0} e^{-k(1-p)} \approx \frac{2F_0}{K_0} e^{-k\sqrt{\frac{2F_0}{K_0}}}.$$

resulting in an exponential distribution for stable cluster density distribution. The above results have an interesting practical interpretation: whenever such an exponential cluster size distribution is observed, it is compatible with a fixed merge and split rate. A problem that a polymer chemist faces is to produce for example a shiny and robust polymer plastic, which requires a specific exponential cluster size distribution. This can be achieved by adding proper amounts of solvants to the mixture to control the parameter F_0 or K_0 and yield the desired exponent value. A similar approach can in fact be used in networking to control merge and split rate, for example through buffer management in opportunistic forwarding schemes, as we will demonstrate in Sec. VII-D.

Another property worth noting in this case is that the exponent of the stationary distribution, which may easily be obtained from a macroscopic observation of the clustering process, is related to the exponent $1/\sqrt{1+2K_0/F_0}$ of time convergence. This is important because the exponent of time convergence is only observable during the transient period of the process; its implications are discussed in the next section.

It is noteworthy that following the approach described in [1] for deriving directly the stationary distribution, will lead to exactly the same distribution as above. The stationary distribution would be obtained by equation 5 where $a(i) = \frac{2F_0}{K_0}$ and the exponent λ is calculated such that the node conservation condition (assuming that $L_1(t) = 1$) is validated (see sec. 2.2 in [1] for more details). This results in a MFA to the stationary distribution

$$\eta(k) = \frac{2F_0}{K_0} e^{-k\sqrt{\frac{2F_0}{K_0}}}$$

that is the same as the asymptotic stationary distribution derived above. However the approach developed in this paper gives access to the transient of the process and in particular the speed of convergence to the stationary distribution.

2) Remarks: Notice that $p(t)$ depends on the ratio $\frac{F_0}{K_0}$ and not on K_0 or F_0 individually. Thus, fragmentation just modifies the probability of the Bernoulli trial and the rate at which $\eta(k,t)$ evolves, but not the Bernoulli nature of the distribution itself. Interestingly, even a very low non-zero split rate stabilizes the cluster distribution.

The pure coagulation solution is recovered in the limit as $F_0 \to 0$, *i.e.*, when $F_0 \to 0$ the above expression for $p(t)$ converges to $\frac{K_0 t}{K_0 t+2}$ as expected from equation 11. By doing a Bernoulli trial with probability p_∞, one can generate clusters following the stationary and stable distribution occurring when split and merge occurs with uniform rates.

We thus solved the specific case with constant merge rate and constant intensity ratio. Unfortunately, the cases of the Smoluchowski equation with analytical solution are rather few (see [6], [7] for an overview). Moreover these cases are of limited practical interest for modeling networks. Therefore, one often has to resort to numerical solution of the Smoluchowski equation.

D. Convergence time and merge–split process timescale

The analysis of the transient behavior of the merge–split process is of interest because it gives deep insight into the temporal evolution of the cluster size distribution. However, often analyzing the transient behavior may be too involved and one is mainly interested in the speed of convergence from the initial state to the stationary state. The convergence time gives a process timescale that is of importance for practical applications as it allows to decide when network composition has stabilized. In order to assess the convergence, we may use as an indicator function $L_0(t) = \sum_{k=1}^{\infty} \eta(k,t)$, which represents the overall number of clusters. By summing up the individual modulated Smoluchowski equations, we obtain an equation for the dynamics of $L_0(t)$ as

$$\frac{\partial L_0(t)}{\partial t} = \sum_{k=0}^{\infty} \sum_{l=0}^{\infty} K'(k,l) \eta(k,t) \eta(l,t),$$

where $K'(k,l)$ is defined in Thm. 1. This shows that the convergence of $L_0(t)$ to its stationary value is controlled by the same term as the Smoluchowski equation.

In the case of constant merge and split rate studied in the previous section, we had $p(t) = 1 - L_0(t)$, yielding

$$L_0(t) - L_0(\infty) = \frac{1 - L_0(\infty)}{1 + \kappa(t)} \left(1 + \frac{r_+}{r_-}\right) e^{-\sqrt{1+\frac{2K_0}{F_0}}t},$$

which means that the convergence of $L_0(t)$ to $L_0(\infty)$ is controlled by the exponent

$$\tau = \frac{1}{\sqrt{1 + \frac{2K_0}{F_0}}}.$$

(see (21) and (22)), which plays the role of the process time scale. If we define that the process has converged if it is at 1% (or 5%) of its stationary distribution, we can expect convergence to happen after 5τ (resp. 3τ) time units. Doing a similar analysis for the purely coalescent case analysed earlier in the paper gives a time scale $\tau = 2/K_0$.

Unfortunately, the convergence time cannot be obtained in closed form for processes where the modulated Smoluchowski equation has no analytical solution and one has to estimate the timescale numerically from the numerical solution of the Smoluchowski equation. This can be achieved by finding the time needed for the system to reach 1% (or 5%) of its stationary value and then dividing this by 5 (resp. 3). Unfortunately, validating this particular aspect against a particular

trace requires that the trace begins in a state where all nodes are isolated as it appears very difficult to reinitialize a scenario to this state. This means that in practice, the transient is typically observed from an initial state that is a deviation from the stationary state. Fortunately, one of the traces we use reaches a state where most nodes are isolated, allowing us to partially validate the above derivation.

V. Node Dynamics

Up to now we analyzed the global state of logical connectivity, however what matters for a particular node is the set of nodes it is logically connected to at every instant of time. Let us suppose that at time t a node belongs to a cluster of size k nodes; then we are interested in the fluctuation of the size of this cluster over time. This will give further insight into the temporal characteristics of the merge–split process. Further, it may serve as an indicator for forwarding decisions of opportunistic forwarding schemes.

The fluctuation of the size of the cluster containing a given node may be derived using the Markov chain structure that was proposed for the merge–split process. From the theory of continuous time markov chains [8], it is well known that the transition probability from state i to state j is given by

$$p_{i,j} = \frac{\sigma_{ij}}{\sum_k \sigma_{ik}},$$

where σ_{ik} is the rate of the transition $i \to k$. Hence, the transition probability from cluster size k to size l is given by:

$$p_{k,l}(t) = \frac{\begin{cases} K(k-l,l)\frac{a(k-l)a(l)}{a(k)}, & 0 < l < k \\ K(k,l-k)\eta(l-k,t), & l > k \end{cases}}{\left(\begin{array}{c} \displaystyle\sum_{m=1}^{\infty} K(k,m)\eta(m,t) \\ \displaystyle + \frac{1}{2}\sum_{m=1}^{k-1} K(k-m,m)\frac{a(k-m)a(m)}{a(k)} \end{array} \right)}. \quad (23)$$

However, this probability is not sufficient to derive the probability for a given node i in a cluster of size k to be in a cluster of size l after the next transition as we need to ensure that node i remains in the cluster of size $l < k$ even if a split event occurs. First, let us assume that the system has converged to its stationary state, meaning that the cluster size distribution is given by the MFA as $\eta(k,t) = \nu(k) = a(k)e^{\lambda k}$ (see (5)). Further, assuming a uniform split between the two fragments, the probability that a node i remains in the fragment of size $l < k$ after its cluster splits into two clusters with sizes $l < k$ and $k - l$, respectively, is given by l/k. Thus we obtain the probability for a given node i in a cluster of size k to find itself in a cluster of size l after the next transition as:

$$p_{k,l} = \begin{cases} \frac{\frac{l}{k}K(k-l,l)a(k-l)a(l)}{S(k)}, & 0 < l < k \\ \frac{K(k,l-k)a(l-k)a(k)e^{\gamma(l-k)}}{S(k)}, & k < l \end{cases} \quad (24)$$

where

$$S(k) = \sum_{m=1}^{\infty} K(k,m)a(m)a(k)e^{-\gamma m} + \frac{1}{2}\sum_{m=1}^{k-1} K(k-m,m)a(k-m)a(m).$$

One must emphasize that the above relation is strictly correct only asymptotically, *i.e.*, when the number of nodes grows without bound, and the correlation between the states of the merge–split process goes to zero. For realistic cases, where the number of nodes in the mobile network, N, is finite, we can approximate the above probability by limiting the infinite series in the numerator to ensure that clusters of size larger than N do not occur and replacing the exponent γ by the exponent $\gamma + \lambda$, where λ is derived as described in [1] such that the node conservation condition (1) holds. This means replacing the term $S(k)$ with

$$S(k) = \sum_{m=1}^{N-k} K(k,m)a(m)a(k)e^{-(\gamma+\lambda)m} + \frac{1}{2}\sum_{m=1}^{k-1} K(k-m,m)a(k-m)a(m)$$

$S(k) = \sum_{m=1}^{N-k} K(k,m)a(m)a(k)e^{-(\gamma+\lambda)m} + \frac{1}{2}\sum_{m=1}^{k-1} K(k-m,m)a(k-m)a(m)$

The approximation improves as the number of nodes increases. While the derivation of the above equation involves quite a few simplifying assumptions, our validation in Sec. VII shows that it provides surprisingly accurate predictions. Note that the above relation assumes that nodes know the size of their cluster. In practice, the cluster size will have to be determined or estimated by the forwarding algorithm, which lies outside the scope of this paper.

A. Connectivity probability between two nodes

Equation (24) provides a way for estimating the probability that a given node i meets a node j in the next transition. This probability is essential for the design of forwarding schemes. A node may for instance decide between storing a message until the next merge event, or dropping it and wait for the source to send another copy, as analyzed in [9].

Assume that at time t, node i has a message for node j. Let node i be in a cluster of size k, while node j is in another cluster. Clearly, a split event will never put node i into the same cluster as node j, hence we are interested in the probability that the next merge event puts node i into the same cluster as node j, allowing those nodes to communicate. This probability can be derived using the above derivation of cluster size fluctuation of the nodes. Suppose that the next event involving the cluster of size k that contains node i is a merge event with a cluster of size l. Assuming that this merge event occurs "randomly", the probability that the cluster of node i merges with that of node j is equal to $\frac{l}{N-k}$; hence the probability of the event that

node i is in the same cluster as node j after the next merge or split event (denoted by $\mathcal{E}(k,i,j)$), is derived as

$$\mathbb{P}[\mathcal{E}(k,i,j)] = \sum_{l=1}^{N-k} \frac{l}{N-k} p_{k,(l+k)},$$

where $p_{k,(l+k)}$ is the probability that the next event is a merge event of the cluster of size k with a cluster of size l, as given in (24).

Of note, the assumption that the merge event is totally random, *i.e.*, the members of the cluster of size l which merges with the cluster of node i are drawn uniformly at random among all nodes, is explained by the phenomenon of propagation of chaos of the mean field, as shown in [1]. Roughly speaking, this means that between two merge or split events a particular node is involved in, there is such a large number of merge and split events between other clusters that the cluster members appear to be distributed uniformly at random. For this assumption to be realistic, the number of nodes in the network needs to be fairly large, implying that the above probability is merely an estimate of what to expect in a real-world scenario and this estimation is expected to become more accurate as the number of nodes grows.

Nonetheless, the above connectivity probability may provide valuable input for opportunistic forwarding schemes.

VI. Model Calibration

In [1], the rationale for the choice of the functional form $q(i,j) = \frac{i^\alpha j^\alpha}{\beta(i+j)^\alpha}$ is given along with a procedure for calibrating the merge–split process by fitting the parameters of the function q to microscopic merge and split rate observable in the mobility pattern of a particular network. Further, we demonstrated that this functional form provides high goodness of fit on real data. Therefore parameters α and β are derived by fitting empirical values of the intensity ratio q to a function $\frac{i^\alpha j^\alpha}{\beta(i+j)^\alpha}$ by a non-linear least-mean-square (LMS) technique. Often, the number of observed merge and split events becomes very small, in particular for large cluster sizes, reducing their statistical value. A weighting equal to $\sqrt{m(i,j)s(i,j)}$ (where $m(i,j)$ is the number of merge events observed between clusters of size i and j and $s(i,j)$ is the number of split events of clusters of size $i+j$ to two clusters of sizes i and j, respectively) is applied to every observed intensity ratio. Moreover, for some cases the dynamical range of the observed intensity ratio $q(i,j)$, is very large, *e.g.*, for small i and j, $q(i,j) \sim 0.001$ and for large i and j, $q(i,j) \sim 10$. In such cases we calibrate $\log q(i,j)$ to $\log \frac{i^\alpha j^\alpha}{\beta(i+j)^\alpha}$.

While the parameters of the function $a(x)$ were enough to analyze the stationary distribution, for the transient behavior we also need to estimate the parameters of the merge rate function $K(i,j)$. We choose the same functional form as for the intensity ratio, *i.e.*, ${i^\alpha j^\alpha}/{\beta(i+j)^\alpha}$. Since the parameters α and β will be different for the merge rate, we use notation α_M (α_R) and β_M (β_R) for the merge (intensity ratio) rate function. This functional form is compatible with clusters being attracted by a gravity force similar to Newtonian gravity with cluster sizes playing the attraction role of mass and the size of the resulting cluster $(i+j)$ being the friction parameter. (The friction parameter in Newtonian gravity is the distance between masses.) In rough terms, the functional form of the merge function can be interpreted as clusters being more attracted to larger clusters but also being repelled by the size of the resulting cluster. The attraction force has a scaling exponent equal to α_M (this is equal to 2 for Newtonian gravity). The nature of the attraction force that drives node clusters to merge is indeed out of the scope of this paper (similar to how the nature of gravity is out of scope of Newtonian mechanics), but one may interpret this force as a result of phenomena such as attractiveness of points of interest, crowds of people, or indeed any imaginable force that motivates people to gather.

Therefore, parameters α_M and β_M are derived by fitting empirically obtained values of merge rate K to a function ${i^{\alpha_M} j^{\alpha_M}}/{\beta_M (i+j)^{\alpha_M}}$ by a non-linear least-mean-square (LMS) technique.

Knowing α_R, β_R, the exponent λ to be used in the mean field approximation is obtained by solving the following equation:

$$\beta_R \sum_{k=1}^{N} \frac{e^{(\lambda)k}}{k^{\alpha_R - 1}} = N \tag{25}$$

Solving this last equation provides all the needed data for predicting the cluster size distribution. We provided in [1] an analysis describing the effect of the parameter values on the shape of the stationary cluster size distribution, showing that for small values of cluster sizes the stationary distribution may be approximated as a polynomial with exponent $-\alpha$, and the number of isolated nodes is estimated as βe^{λ}, where λ depends on the number of nodes while α and β are independent of it. The tail of the distribution is governed partly by the number of nodes, which directly controls λ. Whenever λ becomes positive, one may expect to see a bump on the tail of the distribution. This bump is the sign of emergence of a giant component (a well known phenomenon in the context of percolation theory [10]).

A. Numerical solution of Smoluchowski equation

A more practical issue is that solving the modulated Smoluchowski equation numerically is challenging. For a network with N nodes, the modulated Smoluchowski equation requires solving N non-linear differential equations with N variables. Each of those equations involves all variables, meaning that the system of equations is tightly coupled. This results in a stiff system of differential equations that is computationally intensive even with today's hardware. For example, the 536 nodes scenario of San Francisco taxicab takes four hours of computation to simulate a single day of the evolution of cluster size distribution (using Matlab by Mathworks running on an octocore CPU with 8GB of memory). Processing the 3 millions events to generate cluster size distribution and the fluctuation of the cluster size of individual nodes took the same amount of time. Fortunately, calculating the mean

field approximation and the stationary distribution takes only a couple of seconds. Similarly, the complexity of deriving cluster size transition probabilities from (24) is very low and can be calculated in a split second. In contrast, obtaining the empirical transition probabilities may take several hours for realistic settings.

As shown, the Smoluchowski equation only needs to be solved numerically for the time scale of the process. Therefore, under operational settings, where the stationary distribution, the cluster size transition probabilities, and the node connectivity probabilities are needed, complexity is very low.

In the next section we will validate the theoretical results derived against real-world traces and we will show the application of the theoretical results to opportunistic forwarding.

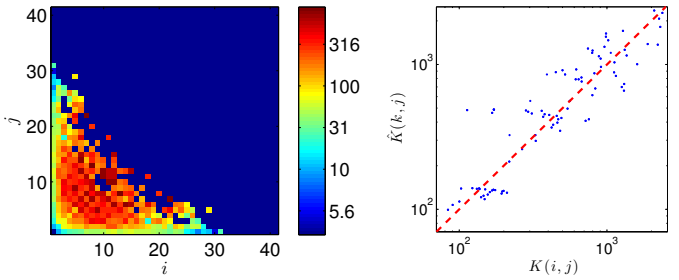

(a) Observed merge rate $K(i,j)$

(b) Predicted $\hat{K}(i,j)$ *vs.* observed merge rate $K(i,j)$

Fig. 1: Observed merge rate $K(i,j)$ and comparison with fitted model in Infocom 2005 scenario

VII. Validation

To verify if the model matches the behavior of realistic mobile networks, we validate it against a contact trace from Infocom 2005 with 41 nodes, a GPS position trace from taxis in San Francisco with 536 nodes, and a similar trace from taxis in Shanghai with 4063 nodes; For all three traces, we showed in [1] the quality of the prediction of the mean field approximation for the stationary cluster size distribution; here we analyze the transient and the time to convergence and dynamics of individual nodes.

A. Infocom 2005 contact trace

The Infocom trace is described in [11]; it comes from 41 attendees of Infocom 2005 carrying Bluetooth contact loggers for three days. The evolution of the connectivity graph over time was reconstructed based on the Bluetooth contacts (logged as tuples `{device address, start time, end time}`), allowing the merge and split rate function to be estimated empirically and their intensity ratios (defined in (2)) to be derived. In [1], we showed that the intensity ratio $q(i,j)$ for this scenario can be fitted by applying the weighted least-mean-squares fitting described in Sec. VI to the observed intensity ratio and yields an estimation of $\hat{\alpha_R} = 3.71 \pm 0.1$, $\hat{\beta_R} = 16.73 \pm 0.95$ with a remarkable $R^2 = 0.998$ goodness of fit indicator. The value $\hat{\lambda} = 0.17$ is obtained by enforcing node conservation, yielding $a(x) = \frac{16.73}{x^{3.71}e^{0.86x}}$.

We applied the same procedure to estimate the merge rate function from the merge rate observed in the trace. This resulted in an estimation $\hat{\alpha_M} = 1.88 \pm 0.02$ and $\hat{\beta_M} = 153.23 \pm 0.26$, with $R^2 = 0.9879$. We plot the observed merge rate $K(i,j)$ and its comparison with the prediction of the fitted model in Fig. 1. Obviously, $K(i,j)$ increases with cluster size; nonetheless, a large part of the rate function remains undefined (shown in blue color on the right hand side of the figure) as no merge events involving these values is observed. The comparison between observed merge and predicted merge rate indicates good agreement with the model, as could be expected by the high value of R^2 given above.

In [1], we found that the mean field approximation fits well the empirical cluster size observed in the Infocom dataset; below we validate the predictive quality of the MFA for transient behavior. In Sec. IV-D, we proposed a convergence criterion based on observing the total number of clusters, yet we also noted that realistic traces do not begin from a disconnected state but rather from a state closer to the stationary state. We solve the modulated Smoluchowski equation parametrized with these values and plot the predicted number of clusters compared with the number observed in the trace in Fig. 2. It is noteworthy that for the Infocom scenario, the experiment began when all participants were close to the booth at which the devices were being distributed; therefore a large cluster (with 38 nodes) formed rather quickly. The transient period and the convergence to stationary state started later when participants moved apart. This is why the transient begins in an initial state with three clusters: one cluster of size 38, one cluster of size 2, and one cluster of size 1, and transitions toward the stationary distribution with 23.56 clusters on average. As can be seen from the figure, the prediction from the mean field approximation is quite good. In particular, the time to converge to stationary state is observed as 7650 seconds (2 hours and 7 minutes). Using the rule of thumb from Sec. IV-D, *i.e.*, finding the time to reach 1% of the stationary value and dividing this by 5, the timescale of the merge–split process describing the Infocom 2005 trace becomes 25 minutes and 30 seconds. This means that a minimal observation window of several times 25 minutes is needed to capture the major characteristics of this process and that after 2 hours and 7 mins the merge–split process loses its memory of the initial state. In particular, after this period the prediction of cluster size fluctuation provided in Sec. V becomes applicable, as will be shown next.

In Fig. 3 we analyse another aspect of the dynamics of the merge-split process: the cluster size transition probabilities of an individual node. The transition probabilities derived with (24) are compared with the empirical values (relative frequency of transitions observed in the trace). The agreement is remarkable; indeed the global goodness of fit coefficient R^2 of the prediction is equal to 0.97. This indicates that if the participants had known the size of their cluster and estimations of the parameter values (α_M, β_M, α_R, β_R and λ) they could have predicted the size of the crowd around them.

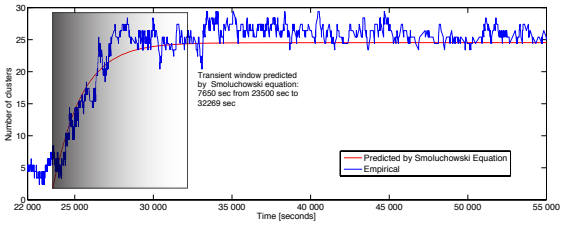

Fig. 2: Transient behavior of the number of clusters $L_0(t)$ for Infocom 2005 scenario

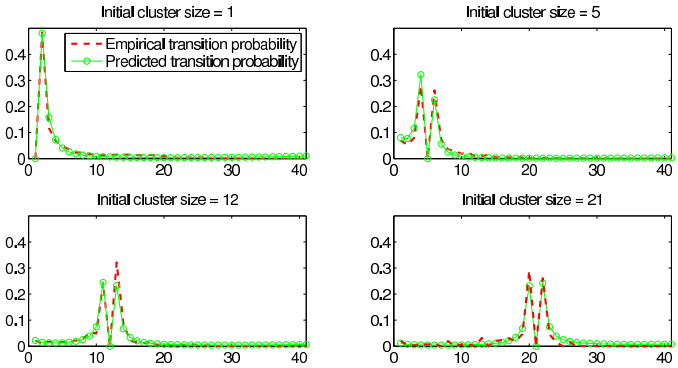

Fig. 3: Probability of cluster size transition for different initial cluster size in the Infocom 2005 scenario

B. Taxicab mobility traces

Since we could not obtain large-scale contact traces with sizable connected components, we resort to mobility traces based on GPS (Global Positioning System) position records from taxicabs. These position reports first need to be translated to a contact process. As is done in other recent publications [12], [13], we use the geometric disc model for connectivity, *i.e.*, there is a link between two nodes if their distance does not exceed a fixed transmission distance, which we set to 200 meters. One caveat is that under this simple propagation model, a link being up between two nodes indicates essentially that those nodes are close enough for communication to be feasible in principle, but it does not guarantee that communication would succeed in practice. (In contrast, in the Infocom contact trace, two nodes are connected only if they actually exchanged data.) However, since the calibration procedure (*cf.* Sec. VI) incorporates the effects from the propagation model similarly as the observed metrics against which we validate the prediction, our validation remains valid.

While one could emulate the effects of wireless propagation post facto, we expect that it would not significantly affect the quality of our prediction. In order to assess the sensitivity of the prediction to the propagation model, we cross-validated parts of the analysis from [1] using a propagation model with path loss and shadow fading; the results are given in [14] and show that, as expected, the propagation model increases the number of link up and down events, but since it affects the calibration in the same way, the prediction quality is similar. Further, in [14] we also analyze the sensitivity to the choice of transmission range in a synthetic random walk scenario with varying coverage.

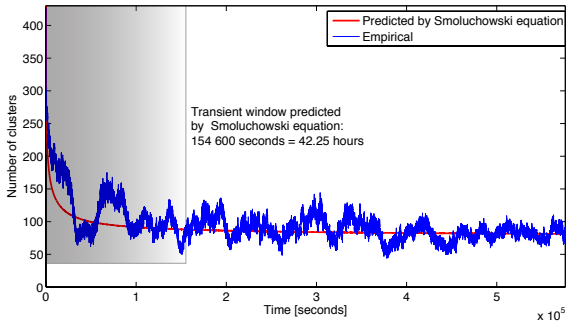

Fig. 4: Transient behavior of the number of clusters $L_0(t)$ observed over 160 hours in San Francisco trace

In order to filter outliers in the GPS position reports, we use an MAD (Median of the Absolute Deviation) filtering procedure [15] on the positions given in the traces. Further, we consider only reports that are no farther apart than certain limits in terms of distance and time. Between those selected reports, we interpolate positions to increase temporal resolution to ten seconds. Finally, to reduce the impact of daily patterns, we consider only the time range 8AM until 12PM.

C. San Francisco taxicab mobility trace

The traces from the San Francisco Cabspotting project have previously been studied in the context of DTN [16]; this trace contains GPS positions from 536 cabs spanning a period of 21 days. Hot spots in this trace are discussed in [16].

We apply the intensity ratio calibration to this trace and obtain estimates of $\hat{\alpha_R} = 4.437 \pm 0.004$ and $\hat{\beta_R} = 133.2 \pm 0.4$, further we get $\hat{\gamma} = 0.3648$ with $R^2 = 0.995$. Applying the node conservation condition yields $\hat{\lambda} = -0.3258$. The merge rate calibration results in $\hat{\alpha_M} = 2.525 \pm 0.008$ and $\hat{\beta_M} = 402.4 \pm 1.3$ with $R^2 = 0.992$. For this trace, in [1] we also showed the quality of the prediction of the MFA for the stationary cluster size distribution; here we now analyze the transient behavior, in particular the time to convergence and the fluctuation of the cluster size of an individual node.

As before, we solve the modulated Smoluchowski equation parametrized with the above values numerically and plot the result in Fig. 4, compared with the empirical result from the trace. The Smoluchowski equation predicts a 1% convergence time of roughly 42 hours (154,600 seconds). Since we do not have results from the convergence period of this trace, the empirical time to convergence cannot be determined exactly. The figure shows that the variability of the empirical curve seems to stabilize at about the value predicted by the Smoluchowski equation and then remains more or less constant during the remaining five days plotted. Applying the rule of thumb described previously, one may state that the timescale of this trace is around 8 hours and 27 minutes. Of note, this timescale is much longer than the one of the Infocom 2005 scenario, which may be explained by the greater freedom of

mobility enjoyed by taxi drivers in San Francisco as compared to the Infocom conference visitors.

Concluding, the timescale of a scenario may indeed be a useful metric for characterizing mobility.

D. Logical Connectivity

The validation so far was concerned with classical connectivity; now we turn to logical connectivity as a function of buffering duration at intermediate nodes. In Sec. II, we introduced the notion of logical connectivity with window D; the implication of this type of logical connectivity is that nodes that are not in the same logical cluster have never had the opportunity to communicate. Let us denote the cluster size vector for logical clusters under this definition by $\nu_N^D(k)$. This enables us to derive the probability that the logical cluster of a given node comprises a fraction of all nodes as a function of window D. Indeed the cluster size vector can be converted to the probability $\mu_N^D(f,t)$ that a message sent by a node may be delivered to a maximum of $f \cdot N$ other nodes. The plots we show are the result of evaluating the following equation for a large number of values in $f = (0.9, 0.99)$ for every buffering duration D:

$$\mu_N^D(f) = \sum_{k=\lfloor fN \rfloor}^{N} \lfloor fN \rfloor \cdot \frac{\nu_N(\lfloor fN \rfloor, \infty)}{N}.$$

1) San Francisco taxicab mobility trace: In Fig. 5a, we plot this probability against f for the San Francisco trace and with window D varying from 10 seconds to 24 hours (86400 seconds).

We observe that for for D in the order of seconds, the probability that a sizable proportion of nodes can be reached is very small, but it increases quickly as D goes toward one minute. Indeed, with increasing D, the number of observed split events decreases and the process converges to a purely coalescent behavior; this can be described by the Smoluchowski equation given in (7). Under these circumstances, a giant component (*i.e.*, a cluster that contains almost all nodes) emerges; in the literature this is called the gelation effect. If a giant component emerges, then almost all nodes in the network have the opportunity to exchange messages at some point in time. In the San Francisco taxicabs scenario, this effect occurs when D reaches about 10 minutes (600 seconds).

We show in Fig. 6 values of parameters α_R and β_R as a function of the window D. It can be seen that with increasing D the parameter β_R, which directly controls the number of isolated node, decreases, *i.e.*, a larger proportion of nodes join clusters. Parameter α_R, which indirectly controls the tail of the stationary state cluster size distribution, increases in absolute value. This means that the proportion of nodes being in large clusters increases. For $D > 600$, no more split events are observed and we have a purely coalescent process with a stationary state distribution of all nodes being in the giant component.

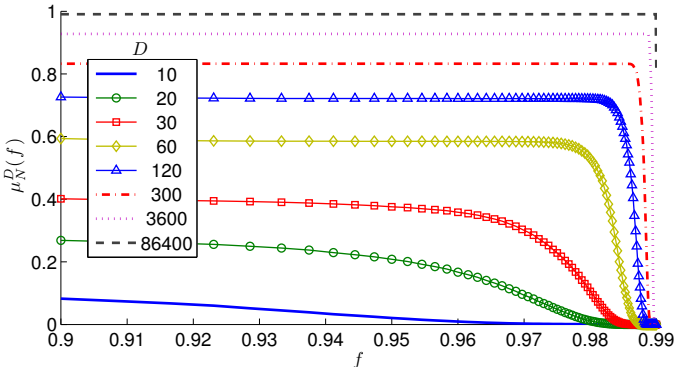

(a) San Francisco

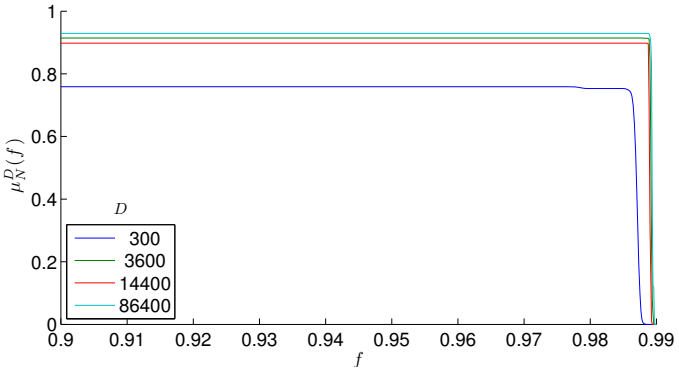

(b) Shanghai

Fig. 5: Probability $\mu_N^D(f)$ that logical cluster size reaches a fraction f of all nodes for various values of window D in seconds

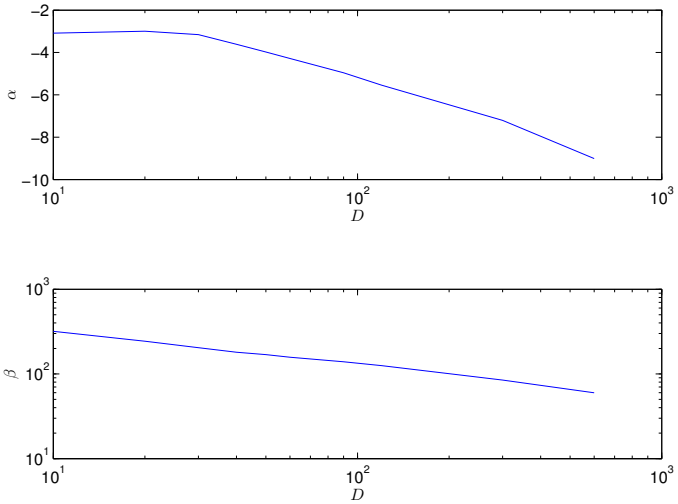

Fig. 6: Variation of α_R and β_R as a function of D in the San Francisco trace

2) Shanghai taxicab mobility trace: The Shanghai taxicab traces were collected by the Traffic Information Grid Team at Shanghai Jiaotong University [17]. This data set contains GPS position reports from 4063 taxis over 28 days. Information about the hot spots in this trace can be found in [18]. The behavior of clustering of this trace in the stationary state

is given in [1]. Due to the large number of nodes, the Smoluchowski equation can not be solved numerically for this trace (see Sec. VI-A). Fortunately, we are able to use this trace in our analysis of logical connectivity, which is based on the mean field approximation.

In Fig. 5b, we show the corresponding plot for Shanghai. Note that due to the computational effort required for every value of D, we only have results for a small number of values. We observe very similar behavior as in the plot for San Francisco taxicabs; however overall one may see that the logical connectivity achieved is consistently lower than that in the San Francisco trace for comparable values of D.

The above analysis shows that opportunistic forwarding between taxicabs may provide almost full connectivity if messages are stored for about ten minutes; indeed, even with a storage duration of one minute, a considerable level of connectivity is reached. Conversely, increasing D further does not increase logical connectivity considerably. Note, however, that the fraction of reachable nodes we study only serves as an upper bound. While the size of the logical cluster, or the fraction of reachable nodes, can only serve as an upper bound, this type of plot nonetheless may serve as a sort of slide rule to gauge the increase in logical connectivity resulting from longer buffering duration. This may help in the design or calibration of a forwarding scheme. Designing a forwarding scheme taking advantage of available connectivity is a challenging problem that lies outside the scope of this paper.

VIII. Related Work

Basic properties such as connectivity have been studied thoroughly through continuum percolation for uniform networks [19] and more recently in clustered scenarios [20]. Observing that connectivity does not give much indication as to the characteristics of a real world scenario, reachability has been proposed as a complementary metric [21], defined as the expected value of the fraction of nodes reachable by a connected path. In the area of complex networks, the clustering behavior has been studied extensively via the clustering coefficient [22]; yet this metric appears to have drawn very limited interest in studies of real world networks.

In terms of space-time paths, [23] found a "small world" behavior in many mobility traces, *i.e.*, the diameter of those networks is in the range of four to six hops. Further to this, [24] observes a "path explosion" phenomenon, describing the observation that after the first space–time path emerges (*i.e.*, the first message is delivered) many more near-optimal paths appear.

At a more abstract level, clustering has been found to be an important characteristic of mobile networks and algorithms building upon this property have been proposed, most of them complementing MANET routing with opportunistic forwarding between clusters (*e.g.*, [25], [26]). Furthermore, some mobility models explicitly produce "realistic" clustering properties (*e.g.*, [26], [27]), based on observed behavior of people. In [16], mobility traces are studied specifically in terms of clustering behavior with a focus on the relationship between cluster size and lifetime. An interesting mobility model is introduce, which deliberately yields node behavior that makes nodes statistically indistinguishable; features realistic clustering behavior. There are similarities in the observations we make; yet we chose to model clustering directly, instead of as a *consequence* of mobility. [28] introduces a temporal distance metric based on the concept of reachability and connected components, aiming to quantify efficiency and diffusion performance of social networks. This work studies more closely the efficiency of contacts by considering the *order* in which they occur. In [13], the existence of a spatial mean field for the age of messages exchanged via a gossip protocol is proved; by a spatial mean field the authors refer to a mean field regime describing the age of the latest update received by mobile nodes. This work is quite similar in methodology to ours, but the model is rather application-oriented.

The phenomenon of a phase transition for asymptotically large networks has been studied already in [19], and more recently been applied to asymptotically large mobile networks (see [10] and references therein). There has also been work on the size of the giant component in the context of complex networks. For instance, [12] studies human mobility using billing records from a mobile phone carrier, accumulating 1.1 billion position reports based on cell tower associations. Not surprisingly, the large amount of data is found to be "computationally untreatable" and scaling is used. In the rescaled data, the emergence of large clusters is observed in urban areas. The authors analyze the size of a giant component *vs.* the transmission range and compare it with the result from a random geometric graph (RGG). This is in analogy to our comparison of the empirical mobility traces with the synthetic random walk model. Similar to our results, they observe that the empirical scenario yields a rather steady increase in the size of the largest component as opposed to the phase transition observed in the RGG.

IX. Conclusion and Future Work

In light of the observation that many real-world networks, such as mobile wireless networks, may be only intermittently connected, or even remain disconnected in the classical definition of connectivity, we introduce the concept of logical connectivity, which defines two nodes as logically connected if the target application may run between them. To analyze in a general fashion both the transient from isolated nodes to logically connected components (clusters) as well as to be able to quantify the level of logical connectivity, we further present the concept of network composition.

In order to analytically study logical connectivity resulting from network composition, we extend the clustering model for mobile wireless networks proposed in [1]. In particular, we use an extension of this model to analyze the transient from an initial state of isolated nodes to the stationary state.

The extensive validation against several real-world traces spanning dozens to thousands of nodes shows that the behavior of a large-scale network may indeed be described accurately as

the resolution of a modified version of the differential equation underlying the merge–split process (known as Smoluchowski equation [5]). Further, we derive an analytical method based on mean field theory to predict the temporal fluctuation of the size of the cluster of individual nodes, yielding important clues for forwarding decisions in opportunistic forwarding schemes. Finally, we apply the concept, the analysis, and the clustering model to a network running an opportunistic forwarding algorithm. In particular, we analyze and quantify its logical connectivity as a function of buffer management used by the forwarding algorithm.

We are currently in the process of applying the methodology to social networks and the Internet topology; those results are to be published in a forthcoming paper.

REFERENCES

[1] S. Heimlicher and K. M. R. Salamatian, "Globs in the primordial soup: The emergence of connected crowds in mobile wireless networks," in *ACM MobiHoc 2010*. Chicago, IL, USA: ACM, Sep. 2010, http://simon.heimlicher.com/_media/publications/heimlicher_globs_mobihoc10.pdf .

[2] E. P. Jones and P. A. Ward, "Routing strategies for delay-tolerant networks," 2006. [Online]. Available: http://ccng.uwaterloo.ca/~pasward/Publications/dtn-routing-survey.pdf

[3] A. H. Marcus, "Stochastic coalescence," *Technometrics*, vol. 10, no. 1, p. 133–143, Feb. 1968. [Online]. Available: http://www.jstor.org/stable/1266230

[4] A. A. Lushnikov, "Coagulation in finite systems," *Journal of Colloid and Interface Science*, vol. 65, no. 2, pp. 276 – 285, 1978. [Online]. Available: http://www.sciencedirect.com/science/article/B6WHR-4CT7DB7-81/2/a9cce2476167883520569312a9b5a922

[5] M. von Smoluchowski, "Drei Vorträge über Diffusion, Brownsche Molekularbewegung und Koagulation von Kolloidteilchen," *Phys. Z.*, vol. 17, p. 557–571 and 585–599, 1916.

[6] R. L. Drake, *A General Mathematical Survey of the Coagulation Equation*, ser. International reviews in aerosol physics and chemistry. Pergamon Press, 1971, vol. 2-3, pp. 201–376.

[7] D. J. Aldous, "Deterministic and stochastic models for coalescence (aggregation, coagulation): a review of the mean-field theory for probabilists," *Bernoulli*, vol. 5, pp. 3–48, 1997.

[8] A. Papoulis, *Probability, Random Variables, and Stochastic Processes*, 2nd ed. New York: McGraw-Hill, 1984.

[9] S. Heimlicher, M. Karaliopoulos, H. Levy, and T. Spyropoulos, "On Leveraging Partial Paths in Partially-Connected Networks," in *INFOCOM 2009*, Apr. 2009.

[10] O. Dousse, *Asymptotic properties of wireless multi-hop networks*. EPFL Ph.D. Thesis no. 3310, 2005.

[11] A. Chaintreau, P. Hui, J. Crowcroft, C. Diot, R. Gass, and J. Scott, "Impact of Human Mobility on the Design of Opportunistic Forwarding Algorithms," in *INFOCOM '06*, Barcelona, Spain, April 2006.

[12] P. Wang, M. C. González, C. A. Hidalgo, and A.-L. Barabasi, "Understanding the Spreading Patterns of Mobile Phone Viruses," *Science*, vol. 324, no. 5930, 2009.

[13] A. Chaintreau, J.-Y. Le Boudec, and N. Ristanovic, "The age of gossip: spatial mean field regime," in *SIGMETRICS '09*, 2009.

[14] S. Heimlicher and K. Salamatian, "Globs in the primordial soup — extended version with proofs," Sep. 2010, http://simon.heimlicher.com/publications/.

[15] L. Davies and U. Gather, "The identification of multiple outliers," *J. Amer. Stat. Assoc.*, vol. 88, no. 423, pp. 782–792, 1993. [Online]. Available: http://www.jstor.org/stable/2290763

[16] M. Piórkowski, N. Sarafijanovoc-Djukic, and M. Grossglauser, "A Parsimonious Model of Mobile Partitioned Networks with Clustering," in *COMSNETS '09*, January 2009.

[17] H.-Y. Huang, P.-E. Luo, M. Li, D. Li, X. Li, W. Shu, and M.-Y. Wu, "Performance evaluation of SUVnet with real-time traffic data," *IEEE Transactions on Vehicular Technology*, vol. 56, no. 6, pp. 3381–3396, Nov. 2007.

[18] J. Lee, K. Lee, J. Jung, and S. Chong, "Performance evaluation of a DTN as a city-wide infrastructure network," in *CFI '09*, 2009. [Online]. Available: http://doi.acm.org/10.1145/1555697.1555717

[19] T. Philips, S. Panwar, and A. Tantawi, "Critical connectivity phenomena in multihop radio models," *IEEE Trans. on Inform. Theory*, vol. 35, no. 5, 1989.

[20] M. A. Serrano and M. Boguñá, "Percolation and epidemic thresholds in clustered networks," *Phys. Rev. Lett.*, vol. 97, no. 8, p. 088701, Aug 2006.

[21] A. Tang, C. Florens, and S. Low, "An empirical study on the connectivity of ad hoc networks," in *IEEE Aerospace Conference*, March 2003.

[22] D. Watts and S. Strogatz, "Collective Dynamics of Small-world networks," *Nature*, vol. 393, pp. 440–442, 1998.

[23] A. Chaintreau, A. Mtibaa, L. Massoulie, and C. Diot, "The diameter of opportunistic mobile networks," in *CoNEXT '07*, 2007.

[24] V. Erramilli, A. Chaintreau, M. Crovella, and C. Diot, "Diversity of forwarding paths in pocket switched networks," in *IMC '07*, 2007.

[25] N. Sarafijanovic-Djukic, M. Piórkowski, and M. Grossglauser, "Island hopping: Efficient mobility-assisted forwarding in partitioned networks," in *IEEE SECON*, 2006.

[26] M. Musolesi and C. Mascolo, "Car: Context-aware adaptive routing for delay-tolerant mobile networks," *IEEE Transactions on Mobile Computing*, vol. 8, 2008.

[27] V. Srinivasan, M. Motani, and W. T. Ooi, "Analysis and implications of student contact patterns derived from campus schedules," in *MobiCom '06*, 2006.

[28] J. Tang, M. Musolesi, C. Mascolo, and V. Latora, "Characterising temporal distance and reachability in mobile and online social networks," *SIGCOMM Comput. Commun. Rev.*, vol. 40, no. 1, pp. 118–124, 2010.